

Activin receptor-like kinase 7 silencing alleviates cardiomyocyte apoptosis, cardiac fibrosis, and dysfunction in diabetic rats

Lin Liu^{1,2}, Xin Zhou^{3,4}, Qiyu Zhang^{5,6}, Li Li^{5,6}, Yuanyuan Shang^{5,6}, Zhihao Wang^{1,2}, Ming Zhong^{5,6}, Yuguo Chen^{3,4}, Wei Zhang^{5,6} and Mengxiong Tang^{3,4} 

¹Department of Geriatric Medicine, Qilu Hospital of Shandong University, Ji'nan 250012, China; ²Key Laboratory of Cardiovascular Proteomics of Shandong Province, Qilu Hospital of Shandong University, Ji'nan 250012, China; ³Department of Emergency Medicine, Qilu Hospital of Shandong University, Ji'nan 250012, China; ⁴Key Laboratory of Emergency and Critical Care Medicine of Shandong Province, Key Laboratory of Cardiopulmonary-Cerebral Resuscitation Research of Shandong Province, Qilu Hospital of Shandong University, Ji'nan 250012, China; ⁵Department of Cardiology, Qilu Hospital of Shandong University, Ji'nan 250012, China; ⁶Key Laboratory of Cardiovascular Remodeling and Function Research, Chinese Ministry of Education and Chinese Ministry of Health, Qilu Hospital of Shandong University, Ji'nan 250012, China
Corresponding author: Mengxiong Tang. Email: mengxiongtang@hotmail.com

Impact Statement

Diabetic cardiomyopathy (DCM) is the primary cause of heart failure in diabetic patients. Cardiomyocyte apoptosis and interstitial fibrosis play important roles in the onset and progression of DCM. Activin receptor-like kinase 7 (ALK7) which is a new member of the type I transforming growth factor- β receptors family has been demonstrated to participate in regulating cell apoptosis. However, the role of ALK7 in the pathogenesis of DCM has not been directly investigated. The current study indicated that ALK7 silencing significantly attenuates cardiomyocyte apoptosis, cardiac fibrosis as well as insulin resistance through mediating Smad2/3 and Akt signaling pathways in a low-dose streptozotocin (STZ)-induced diabetes rat model. This evidence suggests that ALK7 gene silencing might serve as a potential therapeutic approach for DCM.

Abstract

Activin receptor-like kinase 7 (ALK7) is associated with lipometabolism and insulin sensitivity. Our previous study demonstrated that ALK7 participated in high glucose-induced cardiomyocyte apoptosis. The aim of our study was to investigate whether ALK7 plays an important role in modulating diabetic cardiomyopathy (DCM) and the mechanisms involved. The model of diabetes was induced in male Sprague–Dawley rats (120–140 g) by high-fat diet and intraperitoneal injections of low-dose streptozotocin (30 mg/kg). Animals were separated into four groups: control, DCM, DCM with ALK7 silencing, and DCM with vehicle control. The cardiac function was assessed by catheterization. Histopathologic analyses of collagen content and apoptosis rate, and protein analyses of ALK7, Smad2/3, Akt, Caspase3, and Bax/Bcl2 were performed. This study showed a rat model of DCM with hyperglycemia, severe insulin resistance, left ventricular dysfunction, and structural remodeling. With ALK7 silencing, the apoptotic cell death (apoptosis rate assessed by TUNEL, ratio of Bax/Bcl2 and expression of cleaved Caspase3), fibrosis areas, and Collagen I-to-III ratio decreased significantly. The insulin resistance and diastolic dysfunction were also ameliorated by ALK7 silencing. Furthermore, the depressed phosphorylation of Akt was restored while elevated phosphorylation of Smad2/3 decreased after the silencing of ALK7. The results suggest ALK7 silencing plays a protective role in DCM and may serve as a potential target for the treatment of human DCM.

Keywords: Apoptosis, Akt, diabetic cardiomyopathy, diabetes mellitus, fibrosis, Smad2/3

Experimental Biology and Medicine 2022; 247: 1397–1409. DOI: 10.1177/15353702221095049

Introduction

Diabetic cardiomyopathy (DCM), an independent diabetes-associated cardiovascular complication, is typically characterized by left ventricular (LV) early onset diastolic and late onset systolic dysfunction.^{1,2} Multifaceted stimuli such as hyperglycemia, insulin resistance, and lipid accumulation are involved in the onset and progression of DCM.^{3–5} Cardiomyocyte apoptosis and interstitial fibrosis are two major pathological features of DCM and could cause

persistent loss of effective contractile tissue and increased myocardial stiffness both of which inevitably result in cardiac dysfunction.^{6,7} However, the underlying mechanisms by which diabetes leads to apoptosis and fibrosis remain incompletely elucidated.

Activin receptor-like kinase 7 (ALK7), initially discovered in rat brain, is a Type I serine/threonine kinase receptor for transforming growth factor- β (TGF- β) family members.⁸ By conferring responsiveness to the specific ligands,^{9,10} ALK7 participates in regulating cell

differentiation, invasion, phenotypic modulation, proliferation, and apoptosis.^{11–18} Recent studies have shown that the nonsense mutation of ALK7 ameliorates fat accumulation and obesity-induced glucose intolerance and insulin resistance.^{9,19–22} These observations lead to the suggestion that the activation of ALK7 contributes to abnormalities of lipometabolism and insulin sensitivity which are important triggers of DCM.^{3,4,23,24} Our previous study showed that the silencing of ALK7 attenuated high glucose-induced cardiomyocyte apoptosis *in vitro*.²⁵ A recent study also suggested that ALK7 was involved in the development of pathological cardiac hypertrophy.²⁶ However, the role of ALK7 in the pathogenesis of DCM has not been directly investigated on cardiac tissues *in vivo*.

Both Smad2/3 and Akt are crucial downstream mediators of the ALK7 signaling pathway.^{17,25,27,28} Previous findings show that increased phosphorylation of Smad2/3 contributes to LV fibrosis in cardiac ischemia/reperfusion and diabetes.^{29,30} Akt plays a key role in the transduction of insulin signal, and depressed activity of Akt is considered to be a potential inducer of insulin resistance.³¹ Thus, on the basis of the above considerations, we hypothesized that ALK7 participated in the development of DCM through mediating Smad2/3 and Akt pathways.

In the current study, we established the rat model of DCM and used ALK7 gene silencing *in vivo* to elucidate the role of ALK7 in the pathogenesis of DCM. The results indicate that ALK7 gene silencing exerts a protective effect in DCM by reducing cardiac apoptosis and fibrosis.

Materials and methods

Experimental animals

Sixty 5-week-old male Sprague–Dawley rats (120–140 g) were obtained from the experimental animal center (Shandong University of Traditional Chinese Medicine, China). The rats were housed under a 12h/12h light/dark cycle with free access to tap water and food. The investigation adhered to the National Institutes of Health guidelines for care and use of laboratory animals (NIH Publication No. 85–23). All the experimental procedures were approved by the Animal Care Committee of Shandong University.

Induction of diabetes in rats

All rats were fed with normal chow for one week before experiments, and then, fasting blood glucose (FBG) and fasting insulin (FINS) were measured, and insulin sensitivity index (ISI) was calculated ($ISI = \ln(FBG \times FINS)^{-1}$). Meanwhile, intraperitoneal glucose tolerance tests (IPGTTs) and intraperitoneal insulin tolerance tests (IPITTs) were performed. All rats were randomly divided into four groups: control, DCM, DCM + ALK7-siRNA, and DCM + vehicle. The control group received normal chow (77% carbohydrate, 20% protein, 3% fat; HFK Bio-Technology, Beijing, China), and the other three groups were fed with a high-fat (HF) diet (48% carbohydrate, 17.5% protein, 34.5% fat; HFK Bio-Technology, Beijing, China).^{32,33} Four weeks later, jugular blood was sampled, and FBG, FINS, IPGTT, and IPITT were repeated. Rats with insulin resistance were intraperitoneally

injected with streptozotocin (STZ, dissolved in 0.1 mol/L citrate buffer, pH 4.5, Sigma, St. Louis, USA) at the dose of 30 mg/kg just once.^{32,33} The control group received an equal volume of citrate buffer alone. After being injected with STZ for one week, rats with FBG levels exceeding 11.1 mmol/L in two consecutive measurements were used for this study. Rats in the DCM + ALK7-siRNA group and the DCM + vehicle group received either ALK7-siRNA or vehicle treatment via the jugular vein after 12 weeks of diabetes. Adenovirus transfection was repeated after two weeks. Rats were sacrificed after 16 weeks of diabetes (The schematic view for model establishment and the following experiments are shown in the Supplementary Material).

IPGTT and IPITT

IPGTT was performed to assess glucose tolerance. All rats were intraperitoneally injected with 20% glucose solution (1 g/kg) after fasting for 12h, and tail vein blood sampling was performed at the time points of 0, 15, 30, 60, and 120 min. A One-Touch SureStep Glucometer (LifeScan, Milpitas, CA, USA) was used to measure serum glucose. The line graph of glucose level at each time point tested was drawn, and the area under the curve (AUC) was calculated. IPITT was performed to assess insulin sensitivity after rats were fasted for 4h. The insulin solution was intraperitoneally injected (1 unit/kg), the blood was sampled, and serum glucose was measured as previously described.

Blood serum analysis

Jugular vein blood sampling was performed after rats were fasted overnight. FINS level was analyzed using enzyme-linked immunosorbent assay (BeiYinlai Biotech, Wuhan, Hubei, China). Blood serum levels of FBG, total cholesterol (TC), and triglyceride (TG) were determined using Bayer 1650 chemistry analyzer, and then ISI was calculated.

Measurement of blood pressure

The heart rate and systolic and diastolic blood pressure were measured by a noninvasive tail-cuff method using an automatic sphygmomanometer (BP-98A; Softron, Tokyo, Japan). The rats were placed in a plexiglas cage heated at 37°C for 5 min before each measurement.

Evaluation of LV function by cardiac catheterization

LV function was assessed by invasive hemodynamic measurement at the end of this study. Rats were anesthetized, and a pressure tip-catheter filled by fluid was inserted in the right carotid artery and then advanced to LV to record LV pressure-data changes. The LV diastolic function and systolic function were quantified by LV end-diastolic pressure (LVEDP) and LV systolic pressure (LVSP), respectively.

Gene silencing of ALK7

Gene silencing was performed after 12 weeks of diabetes when the LV diastolic dysfunction first appeared as described previously. Rats in the DCM + ALK7-siRNA group

and the DCM + vehicle group received adenovirus harboring ALK7 gene (ALK7-siRNA) with either green fluorescent protein (GFP) or control empty virus (vehicle) with GFP at a dose of 2.5×10^{10} plaque-forming units via jugular vein. Adenovirus transfection was repeated after two weeks, and rats were killed four weeks after the first adenovirus transfer. The following oligoribonucleotides were used to inhibit ALK7 synthesis: 5'-GGUCGUUUGUGAUCAGAAACU-3' and 5'-UUUCUGAUCACAAACGACCUU-3'.

Tissue preparation

Hearts were excised and then weighed after large vessels were trimmed. A LV section was cut off transversely at the midventricular level and fixed in paraformaldehyde (4%). The paraffin-embedded sections (5 μ m) were prepared for histological evaluation. The remaining portion of the LV was rapidly frozen and stored at -80°C for further molecular analysis.

Histology and morphometric analysis

The LV tissue was stained with hematoxylin and eosin (H&E), and it was viewed under a microscope (BX52, Olympus, Japan) with $\times 200$ magnification. Masson's trichrome was used to assess the fibrosis in paraffin-embedded LV sections and collagen fibers stained as dark green were interpreted as a measurement of fibrosis. The LV sections were also stained with 0.5% sirius red (Sigma, St. Louis, MO, USA) at room temperature for 30 min to assess the interstitial and perivascular collagen (PVCA) content. Collagen was stained in an intense red color. The area of myocardial fibrosis was analyzed with Image-Pro Plus 5.0 analysis software (Media Cybernetics, USA). PVCA was excluded from the collagen volume fraction (CVF) measurement. The PVCA area/luminal area (LA) was used to standardize PVCA around vessels of different diameters.

In situ detection of apoptotic cells

In situ terminal deoxynucleotidyl transferase-mediated dUTP nick-end labeling (TUNEL) for apoptotic nuclei was done with the In Situ Apoptosis Detection Kit (S7101, Chemicon International, Billerica, MA, USA) according to the manufacturer's procedures. The apoptotic nucleus was stained brown while a negative nucleus was stained light blue. The percentage of TUNEL-positive nuclei was calculated as the number of TUNEL-positive nuclei/total nuclei $\times 100$.

Immunohistochemical staining

Staining was performed with polyclonal rabbit anti-rat Collagen I and III primary antibodies (Abcam, Cambridge, UK) overnight at 4°C , and then treated with goat anti-rabbit secondary antibody (SP9001, Zhongshan Biotech, Beijing, China) at room temperature for 1 h. The reaction was visualized with the DAB kit, and stained sections were then counterstained with hematoxylin. The immunohistochemical staining was quantified by Image-Pro Plus 5.0 software (Media Cybernetics, USA).

Real-time quantitative reverse transcription polymerase chain reaction (RT-PCR)

The RNA was extracted with trizol agent (Invitrogen, Carlsbad, CA, USA) following the manufacturer's procedures, and the purity was determined by 260/280 ratio. Both reverse transcription and PCR reactions were performed as previously described.²⁵ Sequences of the primers were presented as follows: ALK7, forward 5'-TCATGTGGTCAAGTTTCTCCAA-3' and reverse 5'-AAACGTGTGTTTCATAGCTCGTC-3'; GAPDH, forward 5'-TCTCTGCTCCTCCCTGTTCT-3' and reverse 5'-ATCCGTTACACCGACCTTC-3'. The relative gene expression of ALK7 was calculated with 2(-Delta Delta C (T)) method after adjusting for GAPDH.

Western blot analysis

The protein extraction of LV tissue was treated with cell lysis buffer (Beyotime, Shanghai, China) as previously described.²⁵ A total of 15 μ g protein was separated by 10% sodium dodecyl sulphate (SDS)-polyacrylamide gels and electrophoretically transferred to the polyvinylidene fluoride membranes. The blocking was done with 5% nonfat milk for 2 h, and then membranes were incubated with different rabbit anti-rat primary antibodies, including ALK7 antibody (R&D, Minneapolis, MN, USA), phosphor-Akt (Ser473)/Akt, phosphor-Smad2 (Ser465/467)/Smad2, phosphor-Smad3 (Ser423/425)/Smad3, Bcl-2, Bax and cleaved Caspase3 antibody (Cell Signaling Technology, Beverly, MA, USA), and Collagen I and III antibody (Abcam, Cambridge, UK) overnight at 4°C . The goat-anti-rabbit secondary antibodies (Abcam, Cambridge, UK) were used for incubation at room temperature for 2 h after membranes were washed with Tris buffered saline with Tween-20 (TBST). GAPDH (Cell Signaling Technology, Beverly, MA, USA) was used as the loading control. The ECL kit (Amersham Pharmacia, Piscataway, NY, USA) was used to visualize the blots, and the bands were quantified using ImageJ software (National Institutes of Health, USA).

Statistical analysis

Values were expressed as mean \pm SD. The analyses were performed with SPSS software Version 17.0 (SPSS Inc., Chicago, IL, USA). Differences among groups were explored using one-way analysis of variance (ANOVA). Differences between groups were evaluated by Tukey's post hoc test and independent samples *t*-test. Significance was defined as a value of $P < 0.05$.

Results

ALK7 gene silencing ameliorated insulin resistance and metabolism abnormalities

After a four-week HF diet, the IPGTT and IPITT were performed. The results of IPGTT showed that rats had a significantly higher glucose level at each time point tested after the four-week HF diet than at the baseline ($P < 0.05$; Figure 1(A)). The values of AUC for glucose level over the time points tested also increased significantly after the four-week HF

diet compared with the baseline level ($P < 0.001$; Figure 1(B)). Similarly, the glucose levels of IPITT were elevated by the four-week HF diet (Figure 1(C) and (D)). These data demonstrated the induction of insulin resistance in rats which experienced a four-week HF diet.

Both IPGTT and IPITT were repeated before the rats were killed, and the results showed significantly higher glucose levels in the DCM group than the control group ($P < 0.001$, $P < 0.001$). With ALK7 gene silencing, the glucose level of IPGTT and IPITT decreased significantly compared with the vehicle group ($P < 0.01$, $P < 0.01$; Figure 1(E) and (G)). The AUC for IPGTT and IPITT was also lower in the ALK7-siRNA group than the vehicle group ($P < 0.001$, $P < 0.001$; Figure 1(F) and (H)). In addition, the decreased ISI in the DCM group was restored after ALK7 silencing ($P < 0.001$; Figure 2(A) and (B)). These data demonstrated that ALK7-siRNA treatment ameliorated insulin resistance in diabetic rats.

The rats of the DCM group had increased serum levels of TC, TG, and FBG compared with the control group (Figure 2(C) to (E)). The elevated TC and TG appeared at Week 4 while the FBG increased markedly after the onset of diabetes. The increased levels of TC, TG, and FBG were significantly reduced by the ALK7-siRNA treatment ($P < 0.001$, $P < 0.01$, $P < 0.001$; Figure 2(C) to (E)).

Rats in the DCM group had higher values of heart rate, food intake, water intake, and urine volume than the control group ($P < 0.001$, $P < 0.001$, $P < 0.001$, $P < 0.001$, respectively; Table 1). With ALK7-siRNA treatment, both the water intake and urine volume decreased significantly ($P < 0.01$, $P < 0.01$; Table 1). There was no significant difference in body weight and blood pressure among all groups.

ALK7 gene silencing improved cardiac function in DCM

Cardiac function was measured by cardiac catheterization with a pressure detecting catheter positioned into the LV. After 16 weeks of established diabetes, rats in the DCM group exhibited markedly impaired diastolic function compared with the control group, as indicated by increased LVEDP (7.14 ± 0.90 vs. 23.43 ± 1.81 mmHg, respectively; $P < 0.001$). Decreased LVSP was also shown in the DCM group (109.29 ± 9.78 vs. 88 ± 10.6 mmHg, respectively; $P < 0.01$). This impaired cardiac function was partially restored by ALK7-siRNA treatment. Values of LVEDP in the ALK7-siRNA group were significantly lower ($P < 0.001$) than the vehicle group (Figure 3).

ALK7 gene silencing ameliorated cardiac remodeling in DCM

Both the cardiac mRNA and protein expression of ALK7 were significantly upregulated by diabetes ($P < 0.001$, $P < 0.001$; Figure 7(A) and (B)). The elevated expressions of cardiac ALK7 were significantly downregulated by ALK7 silencing ($P < 0.01$, $P < 0.01$; Figure 7(A) and (B)).

Rats of the DCM group showed significantly larger hearts and higher heart weight to body weight ratio (HW/BW) compared with the control group ($P < 0.001$; Figure 4(Aa)). With

ALK7 treatment, HW/BW decreased significantly in the ALK7-siRNA group compared with the vehicle group (2.82 ± 0.33 vs. 3.19 ± 0.27 mg/g, respectively; $P < 0.05$; Figure 4(B)).

The cross-section staining of H&E showed that rats of the DCM group had dilated ventricle and thickened ventricular wall (Figure 4(Ab)). The cardiomyocytes were compact and well organized in the control group while appearing to be hypertrophic and disorganized in the DCM group (Figure 4(Ac) and (Ad)). With ALK7-siRNA treatment, the myocyte hypertrophy and disorganization, as well as LV dilation and wall thickening, were ameliorated (Figure 4(Ab) to (Ad)). The myocyte sizes were significantly decreased in the ALK7-siRNA group compared with the vehicle group (0.35 ± 0.03 vs. 0.50 ± 0.04 mm², respectively; $P < 0.001$; Figure 4(C)).

ALK7 gene silencing prevented cardiomyocyte apoptosis in DCM

The apoptotic cells were stained in brown by TUNEL as shown in Figure 5(A). The expressions of pro-apoptotic protein cleaved Caspase3, Bax, and anti-apoptosis protein Bcl2 were assessed by western blot. Rats of the DCM group showed a significantly increased cardiomyocyte apoptosis rate ($P < 0.001$; Figure 5(A) and (B)) and protein expression of cleaved Caspase3 and Bax/Bcl2 ($P < 0.001$, $P < 0.001$, respectively; Figure 5(C) to (E)). The apoptotic changes in diabetic heart were blunted by a four-week ALK7-siRNA treatment. Rats of the ALK7-siRNA group showed significantly fewer numbers of TUNEL-positive cardiomyocytes and lower protein levels of cleaved Caspase3 and Bax/Bcl2 than the vehicle group ($P < 0.001$, $P < 0.01$, $P < 0.001$, respectively; Figure 5).

ALK7 gene silencing attenuated diabetes induced cardiac fibrosis

Cardiac fibrosis was examined using Masson's trichrome and sirius red staining. Cardiac tissue of the DCM group showed a diffuse, reticular, pockety, and disorganized collagen network structure in both interstitial (Figure 6(Aa) to (Ac)) and perivascular areas (Figure 6(Ad) to (Af)). The CVF and PVCA/LA were higher in the DCM group than the control group ($P < 0.001$, $P < 0.001$; Figure 6(B) and (C)). With ALK7-siRNA treatment, both the interstitial and PVCA deposition were significantly ameliorated, and the collagen fibers were thinner and more uniform than the vehicle group (Figure 6(A)). Besides, CVF and PVCA/LA reduced significantly after ALK7 gene silencing ($P < 0.01$, $P < 0.001$; Figure 6(B) and (C)).

Furthermore, immunohistochemistry analysis showed that the Collagen I-to-III ratio (Coll-I/Coll-III) was significantly higher in the DCM group than the control group ($P < 0.001$; Figure 6(D) and (E)). However, the elevated value of Coll-I/Coll-III was significantly mitigated by ALK7-siRNA treatment ($P < 0.01$; Figure 6(D) and (E)). Western blot also showed that rats of the ALK7-siRNA group had decreased protein levels of Collagen I and III, and decreased Coll-I/Coll-III compared with the vehicle group ($P < 0.001$, $P < 0.01$, $P < 0.01$; Figure 6(F) to (I)).

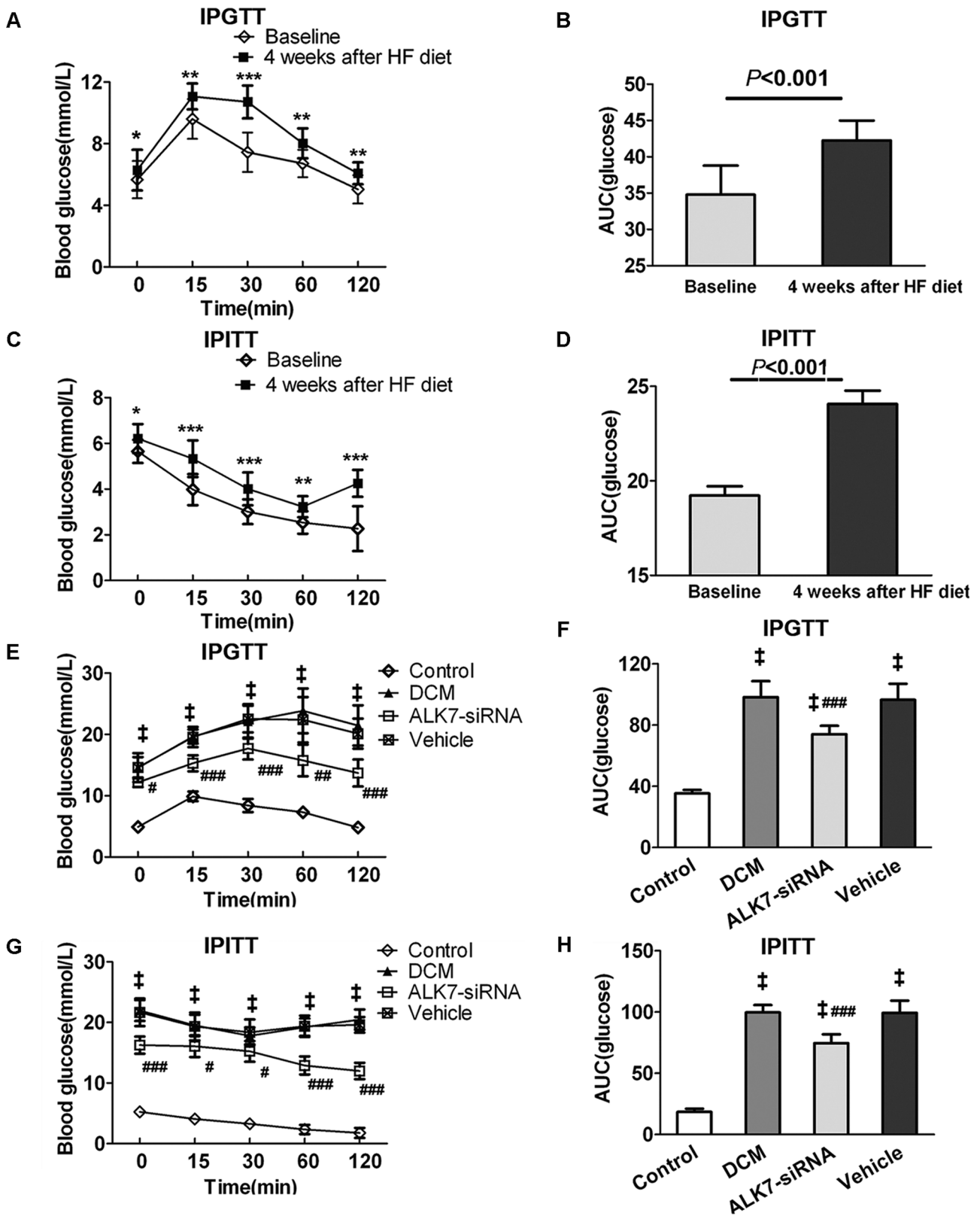


Figure 1. Rats of diabetic cardiomyopathy (DCM) group showed insulin resistance after four-week HF diet and ALK7 silencing ameliorated insulin resistance. (A, C) Intraperitoneal glucose tolerance test (IPGTT) and intraperitoneal insulin tolerance test (IPITT) were performed at baseline and at Week 4 in rats of DCM group. (B, D) Area under the receiver operating characteristic curve (AUC) for IPGTT and IPITT. (E, G) IPGTT and IPITT were repeated at the end of the experiment for all groups. (F, H) AUC for IPGTT and IPITT.

Data are mean \pm SD; $n = 7-10$ per group. HF: high fat.

* $P < 0.05$; ** $P < 0.01$; *** $P < 0.001$ vs. baseline; † $P < 0.001$ vs. control; # $P < 0.05$; ## $P < 0.01$; ### $P < 0.001$ vs. vehicle.

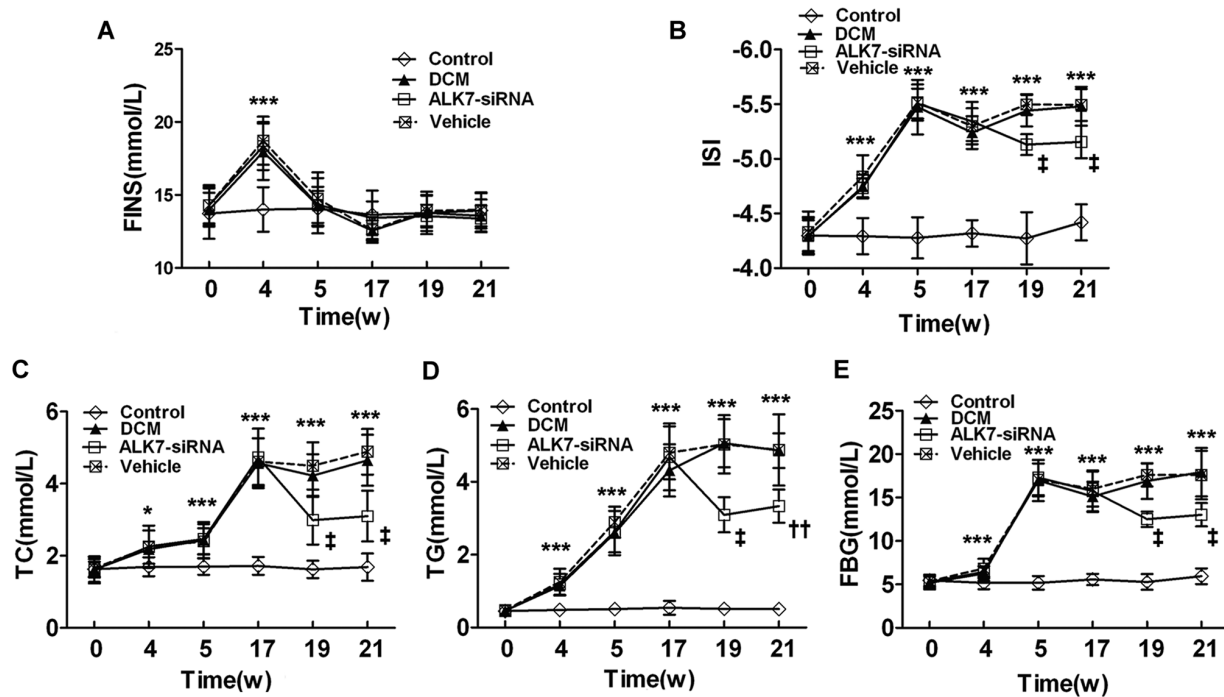


Figure 2. ALK7 gene silencing improved metabolic disturbance. (A) Fasting insulin (FINS). (B) Insulin sensitivity index (ISI). (C) Total cholesterol (TC) levels. (D) Triglyceride (TG) levels. (E) Fasting blood glucose (FBG).

Data are mean \pm SD; $n=7-10$ per group.

* $P < 0.05$; *** $P < 0.001$ vs. control; † $P < 0.01$; ‡ $P < 0.001$ vs. vehicle.

Table 1. Animal characteristics at the end of experiment.

	Control	DCM	ALK7-siRNA	Vehicle
BW (g)	430.38 \pm 20.03	461.25 \pm 27.26	447.14 \pm 33.65	468.5 \pm 35.72
HW (g)	1.13 \pm 0.14	1.47 \pm 0.09***	1.28 \pm 0.10†	1.48 \pm 0.09***
HW/BW(mg/g)	2.58 \pm 0.37	3.18 \pm 0.19**	2.82 \pm 0.33†	3.19 \pm 0.27**
SBP (mmHg)	121.50 \pm 5.95	117.75 \pm 5.94	119.14 \pm 5.96	118.83 \pm 6.21
DBP (mmHg)	92.38 \pm 5.93	91.38 \pm 5.80	93.14 \pm 6.15	92.83 \pm 4.07
MAP (mmHg)	102.05 \pm 5.14	100.17 \pm 5.49	101.81 \pm 3.92	101.50 \pm 3.83
HR (bpm)	324.63 \pm 7.76	343.88 \pm 10.25***	334.29 \pm 11.74	344.33 \pm 15.23*
Food intake (g/day)	16.29 \pm 2.42	28.95 \pm 2.39***	27.14 \pm 2.83***	29.91 \pm 2.84***
Water intake (mL/day)	25.00 \pm 6.99	159.50 \pm 10.03***	131.29 \pm 10.09***†	165.50 \pm 8.64***
Urine volume (mL/day)	19.63 \pm 6.63	132.38 \pm 8.53***	108.14 \pm 10.76***†	134.67 \pm 10.58***

Data are mean \pm SD; $n=7-10$ per group. DCM: diabetic cardiomyopathy; BW: body weight; HW: heart weight; SBP: systolic blood pressure; DBP: diastolic blood pressure; MAP: mean arterial pressure; HR: heart rate.

* $P < 0.05$; ** $P < 0.01$; *** $P < 0.001$ vs. control; † $P < 0.05$, ‡ $P < 0.01$ vs. vehicle.

ALK7 regulated Akt and Smad2/3 signaling pathways

To further elucidate the mechanisms underlying the cardioprotective effects of ALK7-siRNA treatment, we investigated the effects of ALK7 on Smad2/3 and Akt in myocardial tissue. The expression of phosphorylated Akt decreased markedly ($P < 0.001$; Figure 7(C) and (D)) while phosphorylated Smad2/3 increased significantly in the DCM group ($P < 0.001$, $P < 0.001$; Figure 7(E) to (G)). With ALK7 silencing, inhibited phosphorylation of Akt was recovered (Figure 7(C) and (D)), and phosphorylated Smad2 and Smad3 were abolished by 41% and 35%, respectively, in the ALK7-siRNA group (Figure 7(E) to (G)). There was no significant difference of total Smad2/3 and Akt levels in all groups.

Discussion

Although ALK7 activity of the cardiomyocyte is elevated by high glucose,²⁵ its pathophysiological significance in the diabetic heart is incompletely understood. The present study demonstrated a low-dose STZ-induced diabetes rat model with hyperglycemia as well as severe insulin resistance, and this model is considered similar to a Type 2 diabetes model.^{32,33} In this study, the impaired insulin sensitivity, elevated phosphorylation of Smad2/3 and depressed phosphorylation of Akt were restored after ALK7 gene silencing. Furthermore, inhibition of ALK7 ameliorated cardiomyocyte apoptosis and cardiac fibrosis in the diabetes rat model, leading to the improvement of myocardial function. Thus, ALK7 plays a critical role in myocardial remodeling during the

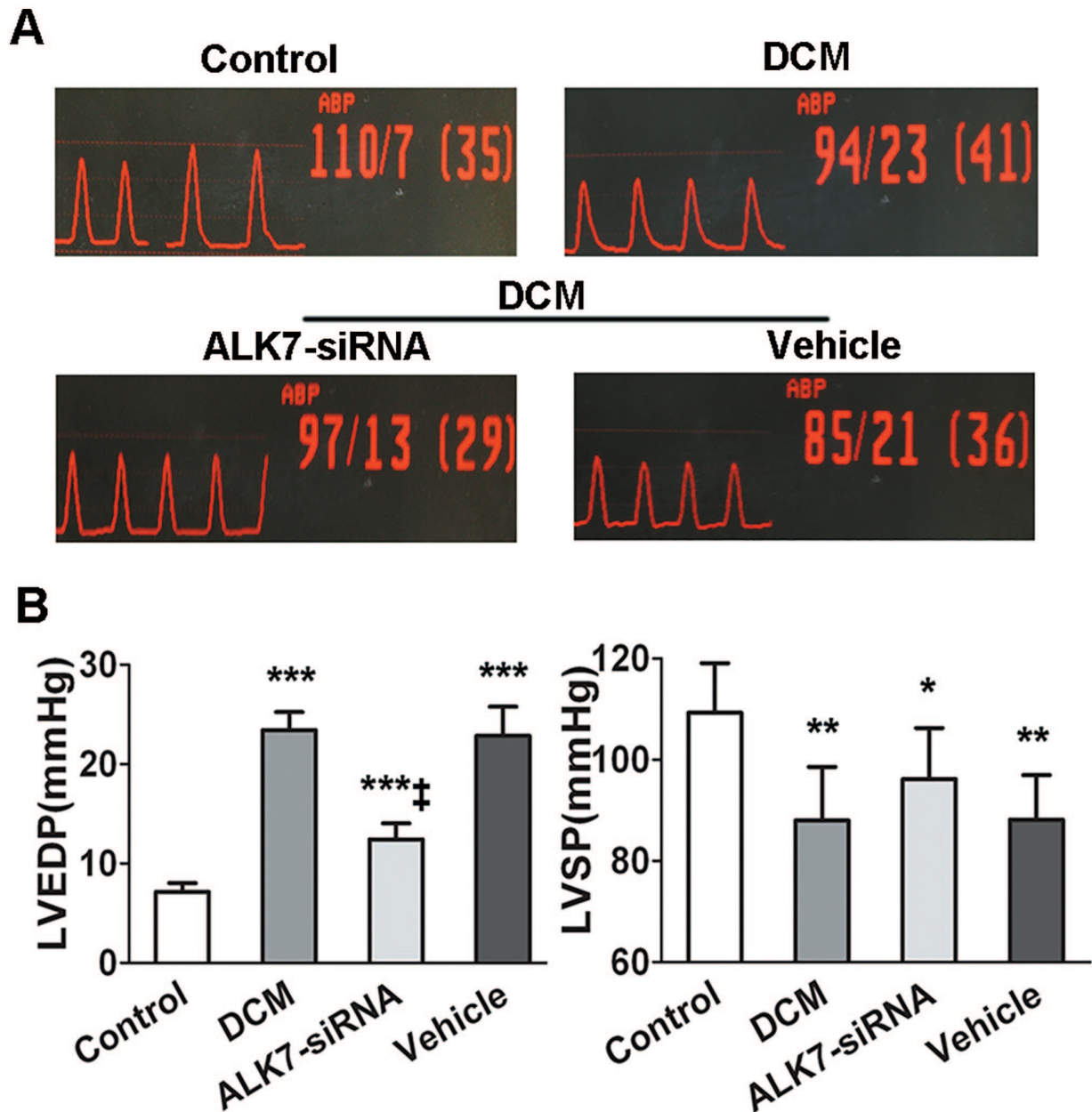


Figure 3. ALK7 silencing ameliorated left ventricular (LV) dysfunction in diabetic rats. (A) Pressure curves of cardiac catheterization. (B) Analysis of LV end-diastolic pressure (LVEDP) LV systolic pressure (LVSP) in all groups.

Data are mean \pm SD; $n=7-8$ per group. (A color version of this figure is available in the online journal.)

* $P < 0.05$; ** $P < 0.01$; *** $P < 0.001$ vs. control; † $P < 0.001$ vs. vehicle.

development of DCM, and this action of ALK7 may be associated with cardiomyocyte apoptosis and cardiac fibrosis in diabetic hearts.

ALK7 gene silencing and cardiomyocyte apoptosis in diabetes

Cardiomyocyte apoptosis is a significant pathological change of DCM. The apoptosis could cause a progressive loss of contractile units, and then initiates cardiac remodeling.⁶ Previous studies demonstrated that ALK7 plays a crucial role in regulating proliferation and apoptosis, such as pancreatic cells, human ovarian epithelial cells, bladder cancer cells, and trophoblast cells.^{11,14,17,18,26,27} Our study in vitro also

proved that ALK7 was involved in high glucose-induced H9c2 cardiomyoblast apoptosis. However, it remains unclear whether ALK7 participates in regulating cardiomyocyte apoptosis in the diabetic hearts.

Consistent with previous studies, we found increased cardiomyocyte apoptosis in the hearts of diabetic rats, correlating with LV dysfunction.^{6,34,35} We further showed that ALK7 silencing ameliorated cardiac apoptosis as well as restored the enhanced phosphorylation of Smad2/3, and depressed phosphorylation of Akt in DCM. Smad2/3 are important apoptosis regulatory proteins.^{36,37} Previous studies demonstrated that ALK7 was a key activator of the Smad2/3 signaling pathway in high glucose-induced pancreatic beta cell and H9c2 cardiomyocyte apoptosis.^{25,27}

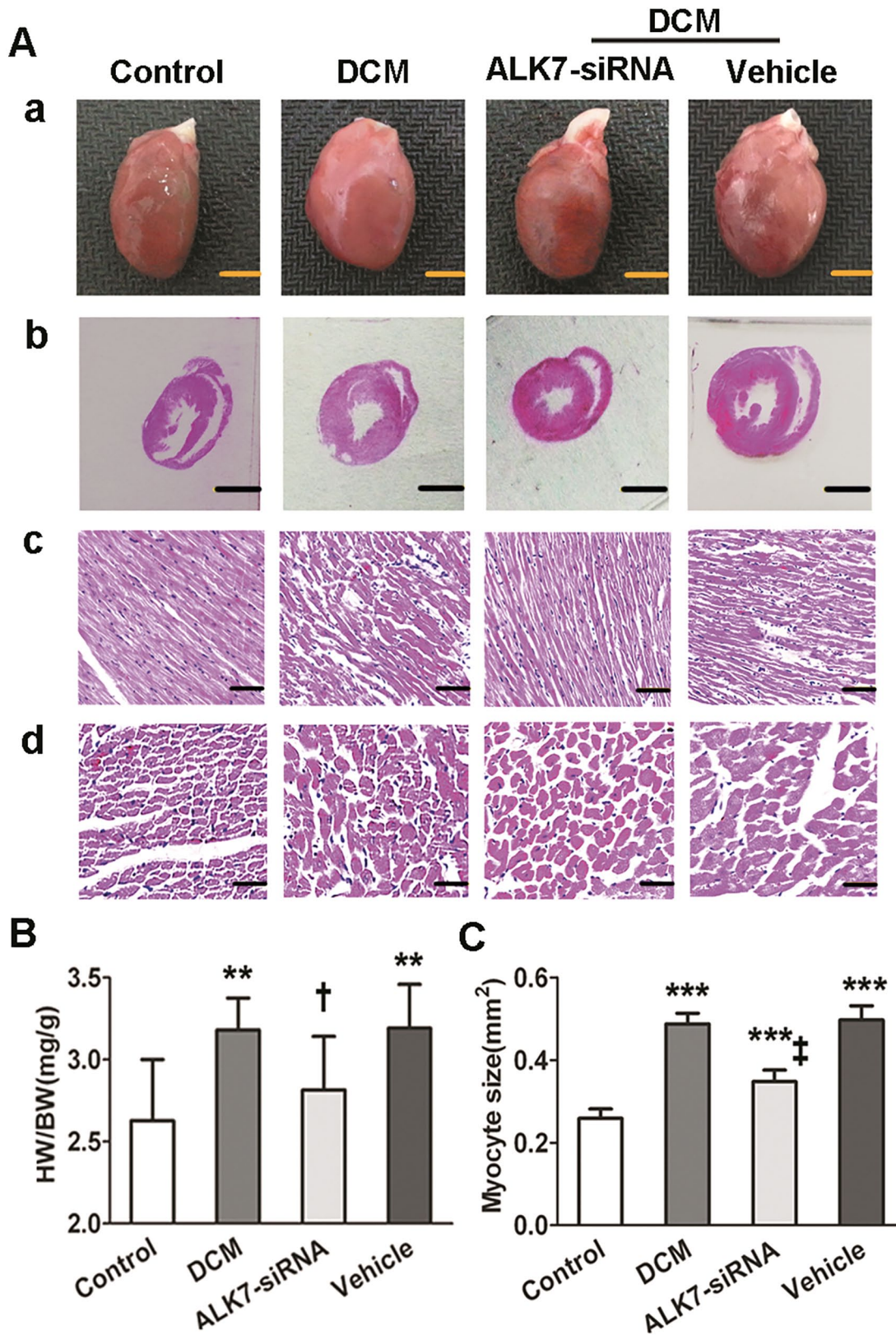


Figure 4. ALK7 gene silencing ameliorated cardiac remodeling in DCM. (Aa). Heart size (scale bar: 5 mm). (Ab). Representative LV cross-section stained with hematoxylin and eosin (H&E) at papillary muscle level (scale bar: 5 mm). (Ac). Longitudinal section of LV stained with H&E (scale bar: 50 μ m). (Ad). Transverse sections of LV stained with H&E (scale bar: 100 μ m). (B). The heart weight-to-body weight ratio (HW/BW). (C) Quantitative analysis of LV cardiomyocyte size. Data are mean \pm SD; $n=7-10$ per group.

** $P < 0.01$; *** $P < 0.001$ vs. control; † $P < 0.05$; ‡ $P < 0.001$ vs. vehicle.

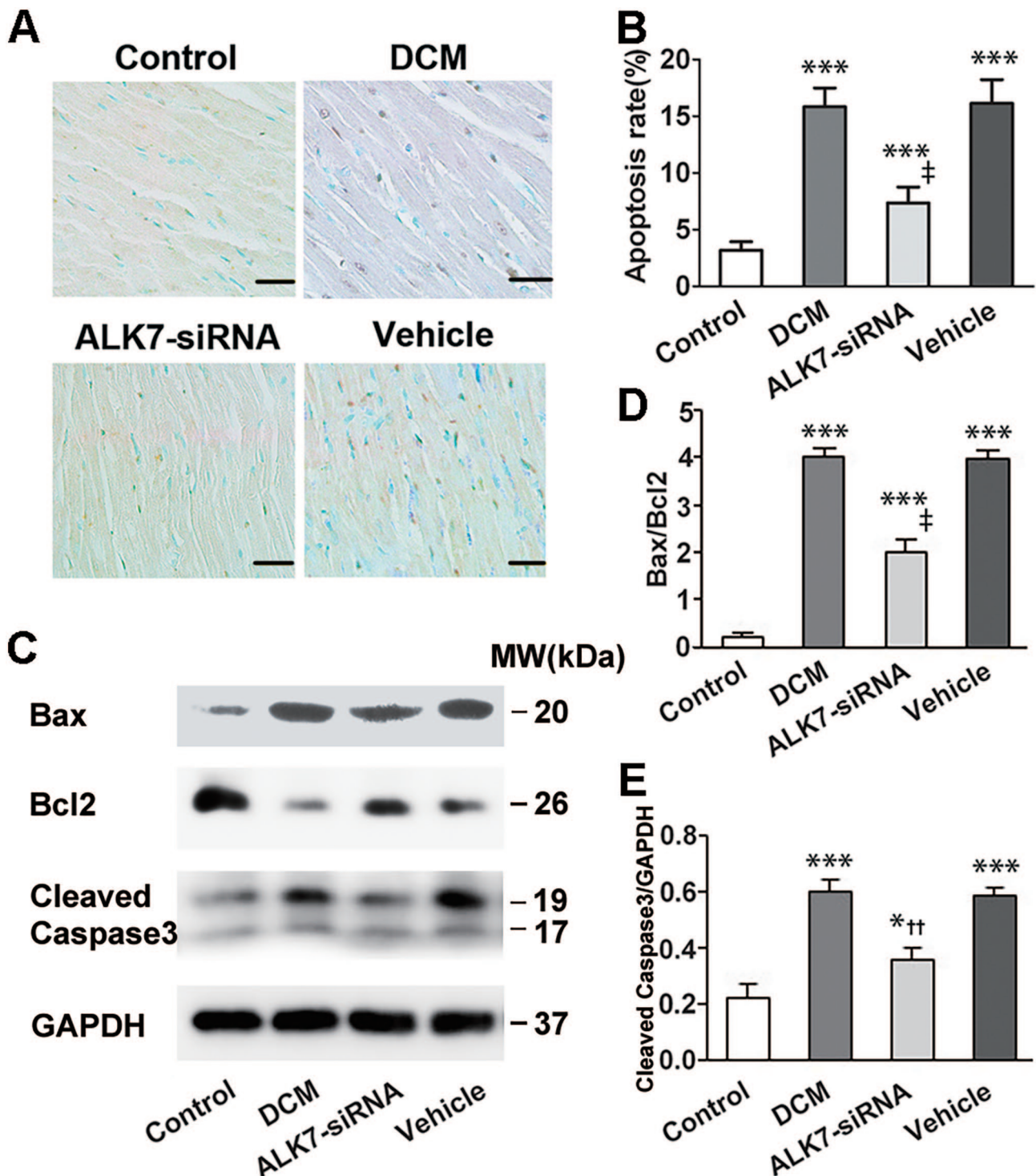


Figure 5. ALK7 silencing attenuated cardiomyocyte apoptosis in diabetic rats. (A) Representatives of TUNEL staining in cardiomyocytes from LV tissues (brown staining considered TUNEL-positive; scale bar: 100 μ m). (B) Quantitative analysis of TUNEL-positive cardiomyocytes ($n=6$ per group). (C) Representative western blot of Bax, Bcl2, and cleaved Caspase3. (D) Western blot analysis of Bcl2-to-Bax ratio (Bcl2/Bax). (E) Western blot analysis of cleaved Caspase3. Values are the mean \pm SD, and western blots were conducted at least 3 times. (A color version of this figure is available in the online journal.) * $P < 0.05$; *** $P < 0.001$ vs. control; †† $P < 0.01$; † $P < 0.001$ vs. vehicle.

We therefore postulated that ALK7 gene silencing decreased the phosphorylation of Smad2/3, thereby directly ameliorating cardiomyocyte apoptosis in diabetic hearts. Akt plays important roles in inhibiting cell apoptosis and promoting cell proliferation.³⁸ The decreased phosphorylation

of Akt restored after ALK7 was silenced, indicated that Akt might be an additional mechanism by which ALK7 mediated apoptosis in DCM. The results were consistent with previous findings that ALK7 participated in elevated glucose-induced pancreatic beta cell apoptosis through

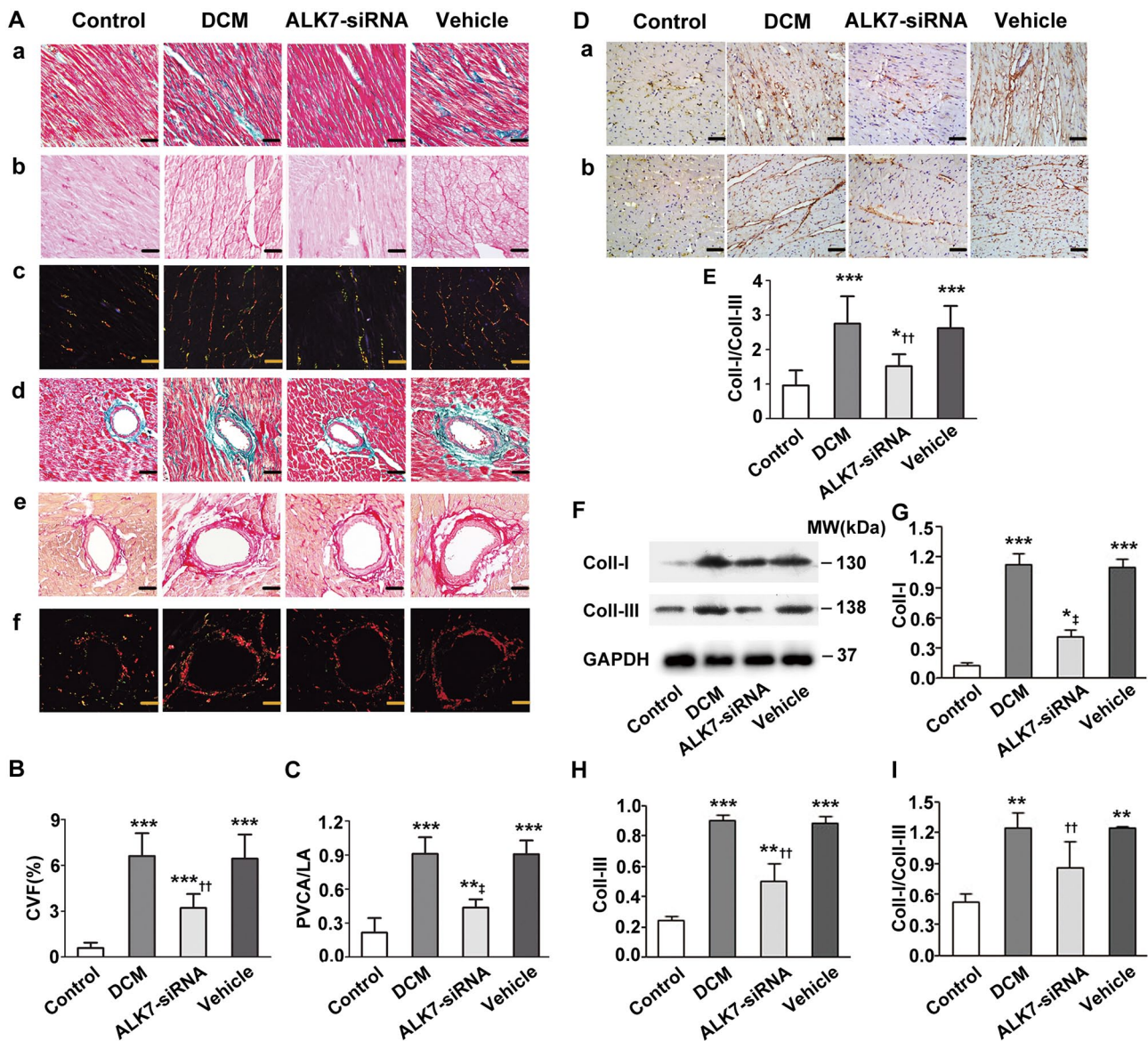


Figure 6. ALK7 gene silencing attenuated cardiac fibrosis in diabetic rats. Aa to Ac: Interstitial fibrosis. (Aa) Representative Masson trichrome staining (collagen fibers is stained green and myocardium is red). (Ab, Ac) Sirius red staining (collagen is stained bright red; Ab: bright-field, Ac: dark-field). Ad to Af: Perivascular fibrosis. (Ad) Masson trichrome staining. (Ae) Sirius red staining (bright-field). (Af) Sirius red staining (dark-field). (B) Quantitative analysis of CVF. (C) Quantitative analysis of PVCA/LA. (D) Representative immunohistochemical staining of Collagen I (Da) and III (Db). (E) Quantitative analysis of Collagen I-to-III ratio (Coll-I/Coll-III). (F) Representative western blot of Coll-I and Coll-III. (G) Western blot analysis of Coll-I. (H) Western blot analysis of Coll-III. (I) Western blot analysis of Coll-I/Coll-III. Scale bar: 50 μ m; Data are mean \pm SD; $n=6$ per group.

* $P < 0.05$; ** $P < 0.01$; *** $P < 0.001$ vs. control; †† $P < 0.01$; ‡ $P < 0.001$ vs. vehicle.

mediating distinct signaling pathways involving Smad2/3 and Akt.²⁷

ALK7 gene silencing and cardiac fibrosis in diabetes

Cardiac fibrosis, characterized by excessive collagen deposition, is another major feature of DCM.⁷ The role of ALK7 in cardiac fibrosis is poorly understood. In the present study, we found that both the interstitial and PVCA deposition was increased in the LV of diabetic rats. ALK7 silencing significantly reduced the aberrant interstitial and PVCA accumulation. The total Collagen I and III content, which constitute 90% of cardiac collagen, decreased significantly,³⁹ in accord

with the improved LV function, especially diastolic function. These findings suggested that ALK7-siRNA treatment prevented cardiac fibrosis in DCM.

Smad2/3 are critical for the fibrosis induced by profibrotic factors, such as advanced glycation end products and Angiotensin II.^{40,41} The phosphorylated Smad2/3 can form a heteromeric complex with co-Smad, and the complex then translocates into the nucleus where they recruit cofactors to Smad-binding element DNA sequences and activate collagen gene transcription.⁴² This study has demonstrated that the phosphorylation of Smad2/3 was influenced by ALK7 activation. These findings therefore confirmed the crucial role of ALK7 in diabetic cardiac fibrosis, and the effects of ALK7 silencing on preventing cardiac fibrosis

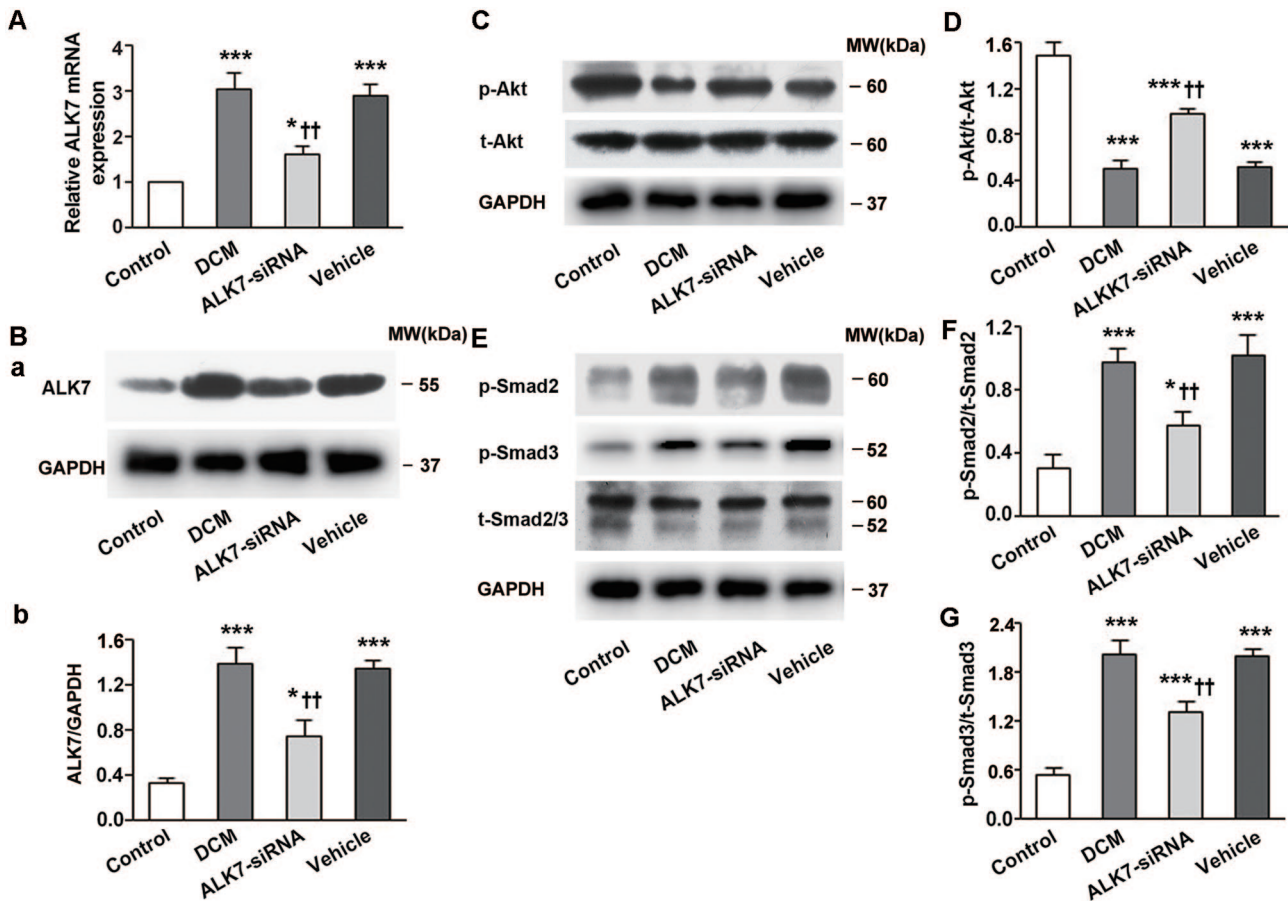


Figure 7. ALK7 silencing restored Akt phosphorylation and suppressed Smad2/3 phosphorylation. (A) Relative ALK7 mRNA expression in all groups. (B) The silencing efficacy of ALK7-siRNA measured by western blot. (C) Representative western blot of p-Akt and t-Akt. (D) Western blot analysis of p-Akt/t-Akt. (E) Representative western blot of p-Smad2, p-Smad3 and t-Smad2/3. (F, G) Western blot analysis of p-Smad2/t-Smad2 and p-Smad3/t-Smad3. Values are the mean \pm SD, and western blots were conducted at least 3 times. * $P < 0.05$; *** $P < 0.001$ vs. control; †† $P < 0.01$ vs. vehicle.

might primarily be attributed to the decreased phosphorylation of Smad2/3.

ALK7 gene silencing and insulin resistance in diabetes

Insulin resistance is an important characteristic of this low-dose STZ-induced diabetes rat model. In this study, with gene silencing of ALK7, the elevated serum levels of TC and TG decreased while impaired ISI was restored, indicating that the ALK7 gene silencing ameliorated insulin resistance in diabetic rats. The improvement of insulin resistance could be attributed to increased phosphorylation of Akt which is a key molecule involved in the maintenance of normal glucose homeostasis.³¹ As this study was an adenovirus mediated systemic knock down model, the inhibition of ALK7 in other organs, such as the liver and adipose tissue, might also lead to the improvement of glucose metabolism and finally contribute to the alleviation of insulin resistance.

In addition to a direct role of ALK7 gene silencing in preventing cardiac fibrosis, the anti-fibrosis effects of ALK7-siRNA treatment might also be partly attributable to the amelioration of insulin resistance, which otherwise stimulates the generation of Collagen I and III in fibroblasts.⁴³ The amelioration of insulin resistance might also cause reduction

in the loss of contractile units and finally improve cardiac function.⁴⁴

ALK7 gene silencing and LV dysfunction in diabetes

In the current study, the 16 weeks untreated diabetic rats showed significantly higher LVEDP and lower LVSP compared with rats in the control group, indicating the development of cardiac dysfunction in Type 2 diabetes. Cardiomyocyte apoptosis plays an important role during this process through causing continuous loss of myocardial contractile units and compensatory cardiomyocyte hypertrophy, both of which lead to hemodynamic overload.⁴⁵ Following apoptotic cell death, the aberrant interstitial and PVCA deposition occurs. The increased collagen deposition then results in enlargement of myocardial fibers, decreased LV compliance, and finally preceding systolic LV dysfunction.^{6,46} Notably, a recent study showed that ALK7 protected against pressure overload-induced cardiac hypertrophy in an aortic banding mice model.²⁶ This result indicates that ALK7 may play different roles in various pathological states, although this requires further exploration.

The present study found that ALK7-siRNA treatment caused decreased LVEDP in the DCM group compared

with the vehicle-control group, indicating the attenuation of LV dysfunction in diabetic rats. This result confirmed the pathophysiological significance of ALK7 activation in diabetic hearts, and the improvement of LV function might be attributed to the inhibition of cardiomyocyte apoptosis and cardiac fibrosis as well as the amelioration of insulin resistance by ALK7 gene silencing.

However, our findings should be seen in the light of some limitations. First, the ALK7 systemic knock down model was used in this study. Second, cardiac catheterization combined with echocardiography allows for a more comprehensive assessment of cardiac function. Further investigations using a cardiac-specific knockout model is required to explore the role of ALK7 in the development of DCM. Despite the above limitations, our study still provides new insights into DCM.

In conclusion, ALK7 silencing significantly attenuates cardiomyocyte apoptosis, cardiac fibrosis, as well as insulin resistance in a low-dose STZ-induced diabetes rat model. These effects of ALK7 may be mediated through Smad2/3 and Akt signaling. The cardioprotective effects with ALK7 gene silencing suggest a potential therapeutic approach for the treatment of DCM in diabetes mellitus.

AUTHORS' CONTRIBUTIONS

All authors participated in the design, carrying out of the study, analysis of the data and review of the manuscript. LL (Lin Liu) researched data and wrote the manuscript. XZ and QZ researched data. LL (Li Li) edited the draft. ZW contributed to the design of the study. YS contributed to analysis of the data. MZ and WZ reviewed and edited the draft. YC edited the draft. MT is the guarantor of this work and designed the study and had access to all data.


DECLARATION OF CONFLICTING INTERESTS

The author(s) declared no potential conflicts of interest with respect to the research, authorship, and/or publication of this article.

FUNDING

The author(s) disclosed receipt of the following financial support for the research, authorship, and/or publication of this article: This study was supported by the National Natural Science Foundation of China (grant number 81670411, 81270352 and 81270287), the Independent Innovation Foundation of Shandong University (grant number 2009TS069), and the Distinguished Young and Middle-aged Scientist Award Foundation of Shandong province (grant number BS2011YY013).

ORCID ID

Mengxiong Tang  <https://orcid.org/0000-0003-4435-7311>

SUPPLEMENTAL MATERIAL

Supplemental material for this article is available online.

REFERENCES

- Poornima IG, Parikh P, Shannon RP. Diabetic cardiomyopathy: the search for a unifying hypothesis. *Circ Res* 2006;**98**:596–605
- Bell DS. Diabetic cardiomyopathy. *Diabetes Care* 2003;**26**:2949–51
- Witteles RM, Fowler MB. Insulin-resistant cardiomyopathy clinical evidence, mechanisms, and treatment options. *J Am Coll Cardiol* 2008;**51**:93–102
- Jia G, Whaley-Connell A, Sowers JR. Diabetic cardiomyopathy: a hyperglycaemia- and insulin-resistance-induced heart disease. *Diabetologia* 2018;**61**:21–8
- Pulinilkunnil T, Kienesberger PC, Nagendran J, Waller TJ, Young ME, Kershaw EE, Korbitt G, Haemmerle G, Zechner R, Dyck JR. Myocardial adipose triglyceride lipase overexpression protects diabetic mice from the development of lipotoxic cardiomyopathy. *Diabetes* 2013;**62**:1464–77
- Qi B, He L, Zhao Y, Zhang L, He Y, Li J, Li C, Zhang B, Huang Q, Xing J, Li F, Li Y, Ji L. Akap1 deficiency exacerbates diabetic cardiomyopathy in mice by NDUF51-mediated mitochondrial dysfunction and apoptosis. *Diabetologia* 2020;**63**:1072–87
- Yue Y, Meng K, Pu Y, Zhang X. Transforming growth factor beta (TGF- β) mediates cardiac fibrosis and induces diabetic cardiomyopathy. *Diabetes Res Clin Pract* 2017;**133**:124–30
- Tsuchida K, Sawchenko PE, Nishikawa S, Vale WW. Molecular cloning of a novel type I receptor serine/threonine kinase for the TGF beta superfamily from rat brain. *Mol Cell Neurosci* 1996;**7**:467–78
- Andersson O, Korach-Andre M, Reissmann E, Ibanez CF, Bertolino P. Growth/differentiation factor 3 signals through ALK7 and regulates accumulation of adipose tissue and diet-induced obesity. *Proc Natl Acad Sci U S A* 2008;**105**:7252–6
- Massague J, Chen YG. Controlling TGF-beta signaling. *Genes Dev* 2000;**14**:627–44
- Cheng WL, Zhang Q, Cao JL, Chen XL, Li W, Zhang L, Chao SP, Zhao F. ALK7 acts as a positive regulator of macrophage activation through down-regulation of PPAR γ expression. *J Atheroscler Thromb* 2021;**28**:375–84
- Gong FH, Cheng WL, Zhang Q, Chen XL, Cao JL, Yang T, Song WH, Zhao F. ALK7 promotes vascular smooth muscle cells phenotypic modulation by negative regulating PPAR γ expression. *J Cardiovasc Pharmacol* 2020;**76**:237–45
- Law J, Zhang G, Dragan M, Postovit LM, Bhattacharya M. Nodal signals via β -arrestins and RalGTPases to regulate trophoblast invasion. *Cell Signal* 2014;**26**:1935–42
- Hu T, Su F, Jiang W, Dart DA. Overexpression of activin receptor-like kinase 7 in breast cancer cells is associated with decreased cell growth and adhesion. *Anticancer Res* 2017;**37**:3441–51
- Zhang N, Kumar M, Xu G, Ju W, Yoon T, Xu E, Huang X, Gaisano H, Peng C, Wang Q. Activin receptor-like kinase 7 induces apoptosis of pancreatic beta cells and beta cell lines. *Diabetologia* 2006;**49**:506–18
- Asnaghi L, White DT, Key N, Choi J, Mahale A, Alkatan H, Edward DP, Elkhamary SM, Al-Mesfer S, Maktabi A, Hurtado CG, Lee GY, Carcaboso AM, Mumm JS, Safieh LA, Eberhart CG. ACVR1C/SMAD2 signaling promotes invasion and growth in retinoblastoma. *Oncogene* 2019;**38**:2056–75
- Li Y, Zhong W, Zhu M, Hu S, Su X. Nodal regulates bladder cancer cell migration and invasion via the ALK/Smad signaling pathway. *Oncotargets Ther* 2018;**11**:6589–97
- Shi Z, She K, Li H, Yuan X, Han X, Wang Y. MicroRNA-454 contributes to sustaining the proliferation and invasion of trophoblast cells through inhibiting Nodal/ALK7 signaling in pre-eclampsia. *Chem Biol Interact* 2018;**298**:8–14
- Yogosawa S, Izumi T. Roles of activin receptor-like kinase 7 signaling and its target, peroxisome proliferator-activated receptor gamma, in lean and obese adipocytes. *Adipocyte* 2013;**2**:246–50
- Yogosawa S, Mizutani S, Ogawa Y, Izumi T. Activin receptor-like kinase 7 suppresses lipolysis to accumulate fat in obesity through downregulation of peroxisome proliferator-activated receptor gamma and C/EBPalpha. *Diabetes* 2013;**62**:115–23
- Balkow A, Jagow J, Haas B, Siegel F, Kilić A, Pfeifer A. A novel cross-talk between Alk7 and cGMP signaling differentially regulates brown adipocyte function. *Mol Metab* 2015;**4**:576–83
- Srivastava RK, Lee ES, Sim E, Sheng NC, Ibáñez CF. Sustained anti-obesity effects of life-style change and anti-inflammatory interventions after conditional inactivation of the activin receptor ALK7. *FASEB J* 2021;**35**:e21759
- Bu Y, Okunishi K, Yogosawa S, Mizuno K, Irudayam MJ, Brown CW, Izumi T. Insulin regulates lipolysis and fat mass by upregulating

- growth/differentiation factor 3 in adipose tissue macrophages. *Diabetes* 2018;**67**:1761–72
24. Ying S, Cao H, Hu H, Wang X, Tang Y, Huang C. Alk7 depleted mice exhibit prolonged cardiac repolarization and are predisposed to ventricular arrhythmia. *PLoS ONE* 2016;**11**:e0149205
 25. Liu L, Ding WY, Zhao J, Wang ZH, Zhong M, Zhang W, Chen YG, Zhang Y, Li L, Tang MX. Activin receptor-like kinase 7 mediates high glucose-induced H9c2 cardiomyoblast apoptosis through activation of Smad2/3. *Int J Biochem Cell Biol* 2013;**45**:2027–35
 26. Huang H, Tang Y, Wu G, Mei Y, Liu W, Liu X, Wan N, Liu Y, Huang C. ALK7 protects against pathological cardiac hypertrophy in mice. *Cardiovasc Res* 2015;**108**:50–61
 27. Zhao F, Huang F, Tang M, Li X, Zhang N, Amfilochiadis A, Li Y, Hu R, Jin T, Peng C, Wang Q. Nodal induces apoptosis through activation of the ALK7 signaling pathway in pancreatic INS-1 beta-cells. *Am J Physiol Endocrinol Metab* 2012;**303**:E132–43
 28. De Silva T, Ye G, Liang YY, Fu G, Xu G, Peng C. Nodal promotes glioblastoma cell growth. *Front Endocrinol* 2012;**3**:59
 29. Vivar R, Humeres C, Ayala P, Olmedo I, Catalan M, Garcia L, Lavandero S, Diaz-Araya G. TGF-beta1 prevents simulated ischemia/reperfusion-induced cardiac fibroblast apoptosis by activation of both canonical and non-canonical signaling pathways. *Biochim Biophys Acta* 2013;**1832**:754–62
 30. Liu JC, Wang F, Xie ML, Cheng ZQ, Qin Q, Chen L, Chen R. Osthole inhibits the expressions of collagen I and III through Smad signaling pathway after treatment with TGF-β1 in mouse cardiac fibroblasts. *Int J Cardiol* 2017;**228**:388–93
 31. Cho H, Mu J, Kim JK, Thorvaldsen JL, Chu Q, Crenshaw EB, Kaestner KH, Bartolomei MS, Shulman GI, Birnbaum MJ. Insulin resistance and a diabetes mellitus-like syndrome in mice lacking the protein kinase Akt2 (PKB beta). *Science* 2001;**292**:1728–31
 32. Danda RS, Habiba NM, Rincon-Choles H, Bhandari BK, Barnes JL, Abboud HE, Pergola PE. Kidney involvement in a nongenetic rat model of type 2 diabetes. *Kidney Int* 2005;**68**:2562–71
 33. Ti Y, Xie GL, Wang ZH, Bi XL, Ding WY, Wang J, Jiang GH, Bu PL, Zhang Y, Zhong M, Zhang W. TRB3 gene silencing alleviates diabetic cardiomyopathy in a type 2 diabetic rat model. *Diabetes* 2011;**60**:2963–74
 34. Kuethe F, Sigusch HH, Bornstein SR, Hilbig K, Kamvissi V, Figulla HR. Apoptosis in patients with dilated cardiomyopathy and diabetes: a feature of diabetic cardiomyopathy. *Horm Metab Res* 2007;**39**:672–6
 35. Tan X, Hu L, Shu Z, Chen L, Li X, Du M, Sun D, Mao X, Deng S, Huang K, Zhang F. Role of CCR2 in the development of streptozotocin-treated diabetic cardiomyopathy. *Diabetes* 2019;**68**:2063–73
 36. Heger J, Warga B, Meyering B, Abdallah Y, Schluter KD, Piper HM, Euler G. TGFbeta receptor activation enhances cardiac apoptosis via SMAD activation and concomitant NO release. *J Cell Physiol* 2011;**226**:2683–90
 37. Yang Q, Ren GL, Wei B, Jin J, Huang XR, Shao W, Li J, Meng XM, Lan HY. Conditional knockout of TGF-βRII /Smad2 signals protects against acute renal injury by alleviating cell necroptosis, apoptosis and inflammation. *Theranostics* 2019;**9**:8277–93
 38. Lawlor MA, Alessi DR. PKB/Akt: a key mediator of cell proliferation, survival and insulin responses. *J Cell Sci* 2001;**114**:2903–10
 39. Spinale FG. Matrix metalloproteinases: regulation and dysregulation in the failing heart. *Circ Res* 2002;**90**:520–30
 40. Khalil H, Kanisicak O, Prasad V, Correll RN, Fu X, Schips T, Vagnozzi RJ, Liu R, Huynh T, Lee SJ, Karch J, Molkentin JD. Fibroblast-specific TGF-β-Smad2/3 signaling underlies cardiac fibrosis. *J Clin Invest* 2017;**127**:3770–83
 41. Li JH, Huang XR, Zhu HJ, Oldfield M, Cooper M, Truong LD, Johnson RJ, Lan HY. Advanced glycation end products activate Smad signaling via TGF-beta-dependent and independent mechanisms: implications for diabetic renal and vascular disease. *FASEB J* 2004;**18**:176–8
 42. Massague J, Seoane J, Wotton D. Smad transcription factors. *Genes Dev* 2005;**19**:2783–810
 43. Gorski DJ, Petz A, Reichert C, Twarock S, Grandoch M, Fischer JW. Cardiac fibroblast activation and hyaluronan synthesis in response to hyperglycemia and diet-induced insulin resistance. *Sci Rep* 2019;**9**:1827
 44. Yang CD, Shen Y, Lu L, Ding FH, Yang ZK, Zhang RY, Shen WF, Jin W, Wang XQ. Insulin resistance and dysglycemia are associated with left ventricular remodeling after myocardial infarction in non-diabetic patients. *Cardiovasc Diabetol* 2019;**18**:100
 45. Foo RS, Mani K, Kitsis RN. Death begets failure in the heart. *J Clin Invest* 2005;**115**:565–71
 46. Mizushige K, Yao L, Noma T, Kiyomoto H, Yu Y, Hosomi N, Ohmori K, Matsuo H. Alteration in left ventricular diastolic filling and accumulation of myocardial collagen at insulin-resistant prediabetic stage of a type II diabetic rat model. *Circulation* 2000;**101**:899–907

(Received December 20, 2021, Accepted March 28, 2022)